Alouette Plasma Resonance Phenomena

by

J. A. Taraonis and F. W. Crawford

March 1968

SU-IPR Report No. 234

Prepared under
NASA Grant NGR 05 020 077

INSTITUTE FOR PLASMA RESEARCH
STANFORD UNIVERSITY, STANFORD, CALIFORNIA

ALOUETTE PLASMA RESONANCE PHENOMENA

by

J. A. Tataronis and F. W. Crawford

NASA Grant NGR 05-020-077

SU-IPR Report No. 234

March 1968

[To be presented at: NATO Advanced Study Institute on Plasma Waves in Space and in the Laboratory, Røros, Norway, April 1968.]

Institute for Plasma Research
Stanford University
Stanford, California

CONTENTS

LIST OF FIGURES

ALOUETTE PLASMA RESONANCE PHENOMENA

by

J. A. Tataronis and F. W. Crawford

Institute for Plasma Research
Stanford University
Stanford, California

ABSTRACT

Following experimental observations of ionospheric "ringing" obtained by the Alouette I topside sounder, it has been established theoretically that a magnetoplasma is capable of ringing at harmonics of the electron gyrofrequency, and at the upper hybrid frequency. This resonance phenomenon arises theoretically from singularities of the plasma Green's function due to the pinching of the real wave-number axis by zeros of the dispersion relation describing the normal plasma modes. Typically, there are three values of the wave-number, $k_\perp$, where pinching occurs: First, at $k_\perp = 0$, second at $k_\perp = \pm \infty$, and third at special values where $0 < k_\perp < \infty$. The last type of ringing does not appear to have been observed either in the ionosphere or in the laboratory. In this paper, a numerical study is made of the three cases to determine the relative strengths of the corresponding ionospheric resonances, and hence to determine which resonances are to be expected in sounder experiments.

1. INTRODUCTION

In recent years, it has been established that strong resonances can be excited in a magnetoplasma. Such resonances have been stimulated in the ionosphere, with the aid of rockets[1,2] and satellites,[3] and in laboratory plasmas.[4] What is generally observed is an oscillatory signal, which we shall term 'ringing', which persists for many periods after subjecting the plasma to a pulse. Ringing can occur at the electron plasma frequency, ω_p, the upper hybrid frequency, ω_H $[\equiv (\omega_p^2 + \omega_c^2)^{1/2}]$ and harmonics of the electron gyrofrequency, $n\omega_c$. Calvert and Goe[5] have summarized the results of ionospheric experiments. Crawford, Harp, and Mantei[4] have given results of laboratory experiments on the stimulation of plasma resonances.

Several theories[6-11] have been presented to explain these resonance effects. Agreement with experimental observations is good in that resonances can be predicted at ω_p, ω_H, and $n\omega_c$. There are, however, other resonances predicted that have not been observed experimentally in either the ionosphere or the laboratory. One such class consists of resonances which can only be excited at an angle oblique to the magnetic field.[12] Another example occurs for a series of special frequencies and wave-numbers when the excitation is perpendicular to the magnetic field.[11]

The purpose of this paper is to make a theoretical study of magnetoplasma resonance phenomena occurring perpendicular to the magnetic field in order to determine the relative strengths of the resonances, and hence to determine which are to be expected experimentally. A one-dimensional, quasistatic theory will be presented in which we follow previous authors,[9-11] and characterize the plasma by a Green's function, $G(\omega,x)$. The spatial and temporal forms of the resonances are then determined by the singularities of $G(\omega,x)$ on the real ω axis. A numerical study has been made of the relative strengths of the electric fields at the various resonances for the case of excitation by a planar dipole charge sheet, and of the current and voltage response for excitation by a pair of permeable planar grids.

2. BASIC EQUATIONS

In this section, we present the equations describing the plasma behavior. The plasma is assumed uniform and infinite, with an isotropic Maxwellian electron velocity distribution,

$$f_0(v_\perp, v_\parallel) = \left(1/2\pi v_t^2\right)^{3/2} \exp\left[-\left(v_\perp^2 + v_\parallel^2\right)/2v_t^2\right] \quad , \tag{1}$$

where v_t $[\equiv (\kappa T_e/m)^{1/2}]$ is the electron thermal speed, and $v_\perp$ and $v_\parallel$ are the components of the electron velocity, $\underset{\sim}{v}$, perpendicular and parallel to the external magnetic field, $\underset{\sim}{B}_0$. Ion motion will be neglected. The basic equations are Poisson's equation,

$$\nabla \cdot \underset{\sim}{E}_1(\underset{\sim}{r}, t) = \rho_s(\underset{\sim}{r}, t) - e\, n_0 \int d\underset{\sim}{v}\, f_1\,(\underset{\sim}{v}, \underset{\sim}{r}, t) \quad , \tag{2}$$

for the fluctuating electric field, $\underset{\sim}{E}_1$, and the linearized Vlasov equation for the lowest order term in the perturbation expansion of the electron velocity distribution,

$$\frac{\partial f_1}{\partial t} + \underset{\sim}{v} \cdot \frac{\partial f_1}{\partial \underset{\sim}{r}} - \frac{e}{m} \underset{\sim}{v} \times \underset{\sim}{B}_0 \cdot \frac{\partial f_1}{\partial \underset{\sim}{v}} = \frac{e}{m} \underset{\sim}{E}_1 \cdot \frac{\partial f_1}{\partial \underset{\sim}{v}} \quad . \tag{3}$$

Here, ρ_s is the external charge density representing the source of the perturbations; $-e$ is the electronic charge; m is the electronic mass, and n_0 $(= n_{e0} = n_{i0})$ is the average charged particle density. We make the quasistatic approximation, rather than using the complete set of Maxwell's equations, and justify this by inference from the laboratory results which show resonances for conditions where the free space wavelength exceeds the plasma dimensions.[4]

We shall assume that the resonances are stimulated by a planar dipole antenna consisting of two uniform, parallel, sheet charges, equal to magnitude but opposite in sign, and oriented along $\underset{\sim}{B}_0$. For this source, we have

$$\rho_s(x,t) = \lim_{a\to 0} q_s(t)\,[\delta(x + a/2) - \delta(x - a/2)] = - f_s(t)\,\frac{d\delta(x)}{dx} \quad , \tag{4}$$

where $f_s(t)$ ($\equiv \lim a q_s(t)$ as $a\to 0$) is the strength of the dipole; $q_s(t)$ is the surface charge density on one sheet; a is the distance between the sheets, δ is the Dirac delta-function, and x is the spatial variable perpendicular to $\underset{\sim}{B}_0$, and hence to the sheets. The planar symmetry implies that the gradient operator, ∇, can be replaced in Eqs. (2) and (3) by $(\partial/\partial x)\,\hat{x}$, where $\hat{x}$ is a unit vector along the x-axis.

To solve Eqs. (2) and (3), we introduce a Fourier transform in space, and a Laplace transform in time,

$$E(k_\perp,\omega) = \int_0^\infty dt \int_{-\infty}^{\infty} dx \exp i(k_\perp x - \omega t)\, E(x,t) \quad , \tag{5}$$

and the inverse transformations,

$$E(x,t) = \int_C \frac{d\omega}{2\pi} \int_{-\infty}^{\infty} \frac{dk_\perp}{2\pi} \exp i(\omega t - k_\perp x)\, E(k_\perp,\omega) \quad , \tag{6}$$

where C is the Laplace contour in the lower half complex ω plane. Substituting Eq. (4) in Eq. (2), and then transforming Eqs. (2) and (3) with respect to x and t, yields after using Eq. (1) for the electron velocity distribution,

$$E(k_\perp,\omega) = \frac{f_s(\omega)}{\epsilon_0\, K(\omega,k_\perp)} \quad , \tag{7}$$

where $f_s(\omega)$ is the Laplace transform of $f_s(t)$ and the relative plasma permittivity perpendicular to the magnetic field is[13]

$$K(\omega,k_\perp) = 1 - \frac{\omega_p^2}{\omega_c^2} \sum_{n=-\infty}^{\infty} \frac{\exp(-\lambda)\, I_n(\lambda)}{\lambda} \frac{n\omega_c}{\omega - n\omega_c} \quad , \tag{8}$$

and λ has been written for $(k_\perp v_t/\omega_c)^2$. Equation (7) is now inverted with the aid of Eq. (6) to yield,

$$E(x,t) = \int_C \frac{d\omega}{2\pi} \exp(i\omega t)\, G(\omega,x)\, f_s(\omega) \quad , \tag{9}$$

$$G(\omega,x) = \int_{-\infty}^{\infty} \frac{dk_\perp}{2\pi} \frac{\exp(-ik_\perp x)}{\epsilon_0 K(\omega,k_\perp)} \quad . \tag{10}$$

The Laplace contour C lies below all singularities of the integrand.

The existence of plasma resonance phenomena can be investigated by examining the limiting form of Eq. (9) as $t \to \infty$. This limit is obtainable by first deforming the contour C into the upper half complex ω plane around the singularities of the kernel, $G(\omega,x)$, and the source function $f_s(\omega)$, and then carrying out the integration along the new contour. The analytic properties of $f_s(\omega)$ depend on the specific source used to stimulate the resonances. For pulse excitation, which we shall assume here, and which has been common experimentally, the source will be an entire function of ω , i.e., free of any singularities. No such statement can be made concerning the analyticity of $G(\omega,x)$. This function is a member of a class of integrals that have the form

$$I(z) = \int_\Gamma \frac{p(z,t)}{q(z,t)}\, dt \quad , \tag{11}$$

where Γ is some contour in the complex t plane. It has been shown[14,15,16] that $I(z)$ is singular at a point $z = z_0$ if two or

more poles of the integrand, i.e., zeros of $q(z,t)$, pinch Γ as z approaches z_0 (see Fig. 1). At the point of pinching in the complex t plane, the derivative $[\partial\, q(z,t)/\partial t]$ is zero. The presence of pinching singularities of $G(\omega,x)$ on the real ω axis is responsible for resonant effects. In what follows the analytic properties of $G(\omega,x)$ will be determined in order to obtain the time-asymptotic behavior of the electric field. This will also enable us to predict the frequencies, and the relative strengths of the resonances.

3. SINGULARITIES OF $G(\omega, x)$

The frequencies at which zeros of $K(\omega, k_\perp)$ pinch the contour of integration of Eq. (10), i.e., the real $k_\perp$ axis, can be obtained by solving the dispersion relation represented by Eq. (8) with $K(\omega, k_\perp) = 0$ for ω as a function of real $k_\perp$. The solutions are shown in Fig. 2. It should be noted that, for a given $k_\perp$, ω is always real. In fact, Bernstein[13] has shown that if the imaginary part of ω is less than zero, and $k_\perp$ is real, then the dispersion relation cannot be satisfied. This implies that $G(\omega, x)$ has no pinching singularities in the lower half complex ω plane. It will be seen from Fig. 2 that $k_\perp$ may also be real for some ranges of real ω. In this situation, poles of the integrand of Eq. (10) are located on the real $k_\perp$ axis, and the integration is no longer defined. Figure 3 shows how the definition of $G(\omega, x)$, is readily extended by deforming the contour of integration ahead of an advancing pole as the imaginary part of ω approaches zero from negative values. However, useful deformation is impossible if ω approaches a frequency where $d\omega(k_\perp)/dk_\perp$ vanishes, since the contour of integration is pinched at such a point. From Fig. 2, we note that $d\omega(k_\perp)/dk_\perp = 0$ at the following points:

(i) $\underline{k_\perp = 0}$ when $\omega = n\omega_c$, $n = \pm 2, \pm 3, \ldots$, and when $\omega = \omega_H$.

(ii) $\underline{k_\perp \text{ finite and nonzero}}$ when $|n|\omega_c < \omega < (|n| + 1)\omega_c$ and $n = 2, 3, \ldots$. This case is not present in every frequency band. If $|n|\omega_c < \left(\omega_p^2 + \omega_c^2\right)^{1/2} < (|n| + 1)\omega_c$, the dispersion curves shown that $d\omega/dk_\perp \neq 0$ for $\omega < |n|\omega_c$ and $0 < k_\perp < \infty$.

(iii) $\underline{k_\perp = \pm \infty}$ when $\omega = n\omega_c$, where $n = \pm 1, \pm 2 \ldots$.

We shall examine the three cases separately to determine what types of singularities are present.

3.1 Pinching at $k_\perp = 0$

The zeros of $K(\omega, k_\perp)$ in the vicinity of the origin in the complex $k_\perp$ plane are obtained by expanding Eq. (8) in a power series about $k_\perp = 0$. For $\omega \approx n\omega_c$, this yields

$$K(\omega, k_\perp) \approx 1 - \frac{\omega_p^2}{\omega^2 - \omega_c^2} - \frac{1}{2^n n!} \frac{\omega_p^2}{\omega_c^2} \frac{n\omega_c}{\omega - n\omega_c} \left(\frac{k_\perp v_t}{\omega_c} \right)^{2(n-1)} , \quad n \geq 2 . \tag{12}$$

If $\omega \approx -n\omega_c$, where $n \geq 2$, the correct form for $K(\omega, k_\perp)$ is obtained by replacing ω in Eq. (12) by $-\omega$. Hence, any resonance found on the positive real ω axis has associated with it a mirror image on the negative axis. For this reason, it is sufficient to restrict our work to positive harmonics of ω_c.

The zeros of Eq. (12) are located at

$$k_{\perp j} = \frac{\omega_c}{v_t} \left[2^n n! \frac{\omega_c^2}{\omega_p^2} \left(1 - \frac{\omega_p^2}{\omega^2 - \omega_c^2} \right) \frac{\omega - n\omega_c}{n\omega_c} \right]^{\frac{1}{2(n-1)}} \exp\left(i \frac{j-1}{n-1} \pi \right) , \tag{13}$$

where $j = 1, \ldots, 2(n-1)$. Since $\omega \approx n\omega_c$, and in the lower half plane, it is convenient to replace ω in Eq. (13) by $[n\omega_c + \delta \exp i\theta]$, where δ is a small expansion parameter, and $-\pi < \theta < 0$. This yields to lowest significant order in δ,

$$k_{\perp j} = \frac{\omega_c}{v_t} \left[\frac{2^n n!}{n\omega_c} \frac{\omega_c^2}{\omega_p^2} \left(1 - \frac{1}{n^2 - 1} \frac{\omega_p^2}{\omega_c^2} \right) \delta \right]^{\frac{1}{2(n-1)}} \exp\left[i \frac{2(j-1)\pi + \theta}{2(n-1)} \right] . \tag{14}$$

Equation (14) implies that there are $2(n-1)$ poles of the integrand of Eq. (10) surrounding the origin in the complex $k_\perp$ plane, with $(n-1)$ of them above the real axis and $(n-1)$ below.

As $\delta \to 0$, and $\omega \to n\omega_c$, the poles converge toward the origin to form a $2(n-1)^{th}$ root of the dispersion relation that pinches the

real axis, and hence the contour of integration, at $k_\perp = 0$.

It is now simple to find the form of $G(\omega,x)$ near $n\omega_c$. Because of the poles surrounding the origin, the most significant contribution to Eq. (10) will come from values of $k_\perp$ near zero. Therefore, an approximation to the integral can be obtained by substituting for the integrand its small argument expansion. Carrying this out, and approximating $\exp(-ik_\perp x)$ by unity gives,

$$G(\omega,x) = -\frac{\alpha}{2\pi\epsilon_0}(\omega - n\omega_c)\int_{-\infty}^{\infty}\frac{dk_\perp}{k_\perp^{2(n-1)} - \alpha K_c(\omega)(\omega-n\omega_c)}$$

$$K_c(\omega) = 1 - \frac{\omega_p^2}{\omega^2 - \omega_c^2} \quad , \quad \alpha = \frac{2^n n!}{n\omega_c}\frac{\omega_c^2}{\omega_p^2}\left(\frac{\omega_c}{v_t}\right)^{2(n-1)} \quad . \qquad (15)$$

It will be noted that $K_c(\omega)$ is the cold plasma relative permittivity component perpendicular to the magnetic field.

The integration in Eq. (15) is accomplished by use of Cauchy's residue theorem, which permits us to write

$$G(\omega,x) = \frac{\alpha}{i\epsilon_0}(\omega-n\omega_c)\sum_j \mathrm{Res}\left[k_{\perp j}^{+}(\omega)\right] \quad , \qquad (16)$$

where the summation extends over the residues of the poles located in the upper half complex plane at $k_{\perp j}^{+}$. Equation (13) gives the positions of all poles near the origin. Those above the real axis are listed in Table 1. It is readily established from Eq. (15) that the residue at $k_{\perp j}$ is $\left[1/2(n-1)k_{\perp j}^{2n-3}\right]$. Substituting this in Eq. (16) , and making use of Table 1, leads to,

Table 1. POLES IN UPPER HALF $k_\perp$ PLANE FOR $\omega \approx n\omega_c$

$\omega_H < n\omega_c$	$k^+_{\perp j} = \left[\alpha\left(1 - \frac{1}{n^2-1}\frac{\omega_p^2}{\omega_c^2}\right)\delta\right]^{\frac{1}{2(n-1)}} \exp\left[i\,\frac{2(j-1)\pi + \theta}{2(n-1)}\right]$, $j = 2, \ldots, n$
$\omega_H = n\omega_c$	$k^+_{\perp j} = \left[\alpha\,\frac{2n\omega_c}{(n^2-1)\omega_c^2}\,\delta^2\right]^{\frac{1}{2(n-1)}} \exp\left[i\,\frac{(j-1)\pi + \theta}{n-1}\right]$, $j = 2, \ldots, n$
$\omega_H > n\omega_c$	$k^+_{\perp j} = \left[\alpha\left(\frac{1}{n^2-1}\frac{\omega_p^2}{\omega_c^2} - 1\right)\delta\right]^{\frac{1}{2(n-1)}} \exp\left[i\,\frac{(2j-1)\pi + \theta}{2(n-1)}\right]$, $j = 1, \ldots, n-1$

$$G(\omega,x) = \frac{\alpha^{\frac{1}{2(n-1)}}}{i\epsilon_0} \times \begin{cases} \dfrac{(\omega - n\omega_c)^{\frac{1}{2(n-1)}}}{2(n-1)\,\beta_1} \displaystyle\sum_{j=2}^{n} \exp\left[-\,i(j-1)\,\frac{2n-3}{n-1}\,\pi\right], & \omega_H < n\omega_c, \\ \dfrac{(\omega - n\omega_c)^{-\frac{n-2}{n-1}}}{2(n-1)\,\beta_2} \displaystyle\sum_{j=2}^{n} \exp\left[-\,i(j-1)\,\frac{2n-3}{n-1}\,\pi\right], & \omega_H = n\omega_c, \\ \dfrac{(\omega - n\omega_c)^{\frac{1}{2(n-1)}}}{2(n-1)\,\beta_3} \displaystyle\sum_{j=1}^{n-1} \exp\left[-\,i(2j-1)\,\frac{2n-3}{2(n-1)}\,\pi\right], & \omega_H > n\omega_c \end{cases}$$

$$\beta_1 = \left(1 - \frac{1}{n^2 - 1}\frac{\omega_p^2}{\omega_c^2}\right)^{\frac{2n-3}{2n-2}} , \quad \beta_2 = \left[\frac{2n\omega_c}{(n^2 - 1)\omega_c^2}\right]^{\frac{2n-3}{2n-2}} , \quad \beta_3 = \left(\frac{1}{n^2 - 1}\frac{\omega_p^2}{\omega_c^2} - 1\right)^{\frac{2n-3}{2n-2}} \tag{17}$$

The finite sums can be closed by use of the identity[17]

$$\sum_{k=1}^{n} \exp(ik\varphi) = \frac{\sin\frac{n\varphi}{2}}{\sin\frac{\varphi}{2}} \exp\left(i\frac{n+1}{2}\varphi\right) , \tag{18}$$

to obtain, finally, the expressions,

$$G(\omega,x) = \frac{\alpha^{\frac{1}{2(n-1)}}}{i\epsilon_0} \times \begin{cases} \frac{1}{\beta_1}\frac{i\exp\left[i\frac{\pi}{2(n-1)}\right]}{2(n-1)\sin\frac{\pi}{2(n-1)}}(\omega - n\omega_c)^{\frac{1}{2(n-1)}}, & \omega_H < n\omega_c , \\ \frac{1}{\beta_2}\frac{i\exp\left[i\frac{\pi}{2(n-1)}\right]}{2(n-1)\sin\frac{\pi}{2(n-1)}}(\omega - n\omega_c)^{-\frac{n-2}{n-1}}, & \omega_H = n\omega_c , \\ \frac{1}{\beta_3}\frac{-i}{2(n-1)\sin\frac{\pi}{2(n-1)}}(\omega - n\omega_c)^{\frac{1}{2(n-1)}}, & \omega_H > n\omega_c . \end{cases} \tag{19}$$

Clearly, there are singularities at $n\omega_c$ ($n = 2,3, \ldots$). When $\omega_H \neq n\omega_c$, the singularities are branch points. They are replaced by branch poles when ω_H is identical to $n\omega_c$. An exception to the rule occurs when $n = 2$. In this case, $G(\omega,x)$ is regular, and no resonance is predicted.

In addition to the singularities found so far, there is one at ω_H. The form of $G(\omega,x)$ near this point is determined by the power series expansion of $K(\omega,k_\perp)$. For $\omega \approx \omega_H \neq n\omega_c$, this has the form, to lowest significant order in $k_\perp$,

$$K(\omega, k_\perp) \approx \frac{2\omega_H}{\omega_p^2}(\omega - \omega_H) - \left(\frac{3\omega_c^2}{\omega_p^2 - 3\omega_c^2}\right)\left(\frac{k_\perp v_t}{\omega_c}\right)^2 \quad . \tag{20}$$

The zeros of $K(\omega, k_\perp)$ can be obtained by substituting for ω the expression $(\omega_H + \delta \exp i\theta)$, where $-\pi < \theta < 0$. This yields

$$k_\perp = \begin{cases} \pm \left[\frac{2}{3}\frac{\delta\omega_H\left(\omega_p^2 - 3\omega_c^2\right)}{\omega_p^2 v_t^2}\right]^{1/2} \exp\left(i\frac{\theta}{2}\right) , & \omega_p^2 > 3\omega_c^2 , \\ \pm i\left[\frac{2}{3}\frac{\delta\omega_H\left(3\omega_c^2 - \omega_p^2\right)}{\omega_p^2 v_t^2}\right]^{1/2} \exp\left(i\frac{\theta}{2}\right) , & \omega_p^2 < 3\omega_c^2 . \end{cases} \tag{21}$$

These roots pinch the real axis as $\delta \to 0$. Taking the residues gives for $\omega \approx \omega_H$,

$$G(\omega, x) = \begin{cases} i\frac{\gamma_1}{2\epsilon_0}\frac{1}{(\omega - \omega_H)^{1/2}} , & \omega_p^2 > 3\omega_c^2 , \\ -\frac{\gamma_2}{2\epsilon_0}\frac{1}{(\omega - \omega_H)^{1/2}} , & \omega_p^2 < 3\omega_c^2 , \end{cases}$$

$$\gamma_1 = \left[\frac{\omega_p^2\left(\omega_p^2 - 3\omega_c^2\right)}{6\omega_H v_t^2}\right]^{1/2} , \quad \gamma_2 = \left[\frac{\omega_p^2\left(3\omega_c^2 - \omega_p^2\right)}{6\omega_H v_t^2}\right]^{1/2} \tag{22}$$

A branch pole is clearly evident at ω_H.

3.2 Pinching at $0 < k_\perp < \infty$.

Figure 2 shows branches of the form illustrated in Fig. 4, for which there are two points, (ω_0 , k_0) and $(\omega_0 , -k_0)$, where $(d\omega/dk_\perp)$ vanishes. If $\partial K(\omega,k)/\partial\omega \neq 0$ at these points, it is implied that $\partial K(\omega,k_\perp)/\partial k_\perp = 0$. This condition is satisfied for the Maxwellian, for all ω and $k_\perp$, since Eq. (8) gives,

$$\frac{\partial K(\omega,k_\perp)}{\partial\omega} = \frac{\omega_p^2}{\omega_c^2} \sum_{n=-\infty}^{\infty} \frac{\exp(-\lambda)\ I_n(\lambda)}{\lambda} \frac{n\omega_c}{(\omega - n\omega_c)^2} > 0 \quad . \tag{23}$$

If, as indicated in Fig. 4, the dispersion relation has only a double root at k_0 for $\omega = \omega_0$, it is readily established that $\partial^2 K(\omega_0 , k_0)/\partial k_\perp^2 = \partial^2 K(\omega_0 , -k_0)/\partial k_\perp^2 > 0$. Hence, the Taylor series expansion of $K(\omega,k_\perp)$ about the point (ω_0,k_0) yields,

$$K(\omega,k_\perp) \approx \frac{\partial K(\omega_0,k_0)}{\partial\omega} (\omega - \omega_0) + \frac{1}{2} \frac{\partial^2 K(\omega_0,k_0)}{\partial k_\perp^2} (k_\perp - k_0)^2 \quad . \tag{24}$$

Since ω is in the lower half plane we substitute $[\omega_0 + \delta\exp i\theta]$, with $-\pi < \theta < 0$, and determine the roots of Eq. (24) for $K(\omega,k_\perp) = 0$. We find two zeros on opposite sides of the real axis at

$$k_\perp = k_0 \pm i \left[\frac{2\delta\ \partial K(\omega_0,k_0)/\partial\omega}{\partial^2 K(\omega_0,k_0)/\partial k_\perp^2} \right]^{1/2} \exp i\frac{\theta}{2} \quad , \tag{25}$$

which converge to k_0 as $\delta \to 0$, to form a double root that pinches the contour of integration of Eq. (10). Similarly, there exist two zeros of $K(\omega,k_\perp)$ near $(-k_0)$ which behave identically to those in Eq. (25) and are located at

$$k_\perp = -k_0 \pm i\left[\frac{2\delta\,\partial K(\omega_0,k_0)/\partial\omega}{\partial K(\omega_0,k_0)/\partial k_\perp^2}\right]^{1/2} \exp i\frac{\theta}{2} \quad . \tag{26}$$

Thus, for $\omega \approx \omega_0$, residue evaluation of Eq. (10) yields

$$G(\omega,x) \approx \frac{2\cos k_0 x}{\epsilon_0\left[2(\partial K/\partial\omega)(\partial^2 K/\partial k_\perp^2)\right]^{1/2}} \frac{1}{(\omega-\omega_0)^{1/2}} \quad , \tag{27}$$

and reveals a branch pole at ω_0 . The partial derivatives in this expression are evaluated at the point (ω_0,k_0) .

3.3 Pinching at $k_\perp = \pm\infty$.

It is clear from Fig. 2 that $d\omega(k_\perp)/dk_\perp \to 0$ as $k_\perp \to \pm\infty$. Therefore, pinching should be expected in this small wavelength limit. There are, however, effects ignored in our theory that would wash out any resulting singularities. One such effect is electron/neutral collisions. When these are taken into account,[18] it is found that the solutions of the dispersion relation indicate $k_\perp$ complex for ω real. The real parts of the solutions for $k_\perp$ effectively follow the collisionless solutions, while the imaginary parts tend towards infinity as the real part of $k_\perp$ approaches infinity. This implies that any singularity in $G(\omega,x)$, due to pinching of the contour of integration at $k_\perp = \infty$ in a collisionless plasma, will move far into the upper half complex ω plane when collisions are introduced. Any resonance that may be excited will be very heavily damped, and unobservable experimentally. In any case, short wavelength effects predicted by the theory are non-physical, They should be rejected whenever the wavelength is smaller that a Debye length. With these considerations in mind, the predicted resonances due to pinching at $k_\perp = \pm\infty$ will not be considered further.

4. ASYMPTOTIC BEHAVIOR OF THE ELECTRIC FIELD

The asymptotic form of the electric field can now be obtained from Eq. (9) by deforming the Laplace contour in the usual manner around the singularities of $G(\omega,x)$ located in Section 3. As $t \to \infty$, Eq. (9) reduces to

$$E(x,t) \sim \sum_k \int_{\Gamma_k} \frac{d\omega}{2\pi} \exp(i\omega t)\, G(\omega,x)\, f_s(\omega) \quad , \tag{28}$$

where the summation is over the branch points of $G(\omega,x)$, and the contour Γ_k extends around the k^{th} branch cut, as shown in Fig. 5. We now examine the k^{th} term in Eq. (28) at each branch point.

4.1 $\omega = n\omega_c$.

Since the contribution to the integral from the part of Γ_k in the upper half complex plane vanishes exponentially as $t \to \infty$, it is sufficient to expand the integrand about $\omega = n\omega_c$ and retain only the most significant parts. Hence, in this limit, the k^{th} term of Eq. (28) approaches, for $\omega_H < n\omega_c$,

$$E_k(x,t) = \frac{\alpha^{\frac{1}{2(n-1)}}\, f_s(n\omega_c)}{\epsilon_0 \beta_1} \frac{\exp\left[in\omega_c t + i\frac{\pi}{2(n-1)}\right]}{2(n-1)\sin\frac{\pi}{2(n-1)}} I_k \quad ,$$

$$I_k = \int_{\Gamma_k} \frac{d\omega}{2\pi} \exp[i(\omega - n\omega_c)\, t]\, (\omega - n\omega_c)^{\frac{1}{2(n-1)}} \quad , \tag{29}$$

where use has been made of Eq. (19), and Γ_k is shown in Fig. 6. The integration, I_k, along Γ_k can be written as a sum of three terms: $[I_{AB} + I_{BCD} + I_{DE}]$. It can readily be shown that as $\delta \to 0$, $I_{BCD} \to 0$. Hence we have,

$$I_k = I_{AB} + I_{DE} = - \frac{\exp[-i\pi/4(n-1)]\ \sin[\pi/2(n-1)]\ \Gamma\left(\frac{2n-1}{2n-2}\right)}{\pi\ t^{\frac{2n-1}{2n-2}}} , \quad (30)$$

where I_{AB} and I_{DE} are evaluated with the identity[17]

$$\int_0^\infty dx\ x^p \exp(-qx) = \frac{\Gamma(p+1)}{q^{p+1}} , \quad (q > 0;\ p + 1 > 0) , \quad (31)$$

and $\Gamma(z)$ is the gamma function. After combining Eqs. (29) and (30), we find that the component of the electric field at $\omega = n\omega_c$ is, as $t \to \infty$,

$$E_k(x,t) = - \frac{\alpha^{\frac{1}{2(n-1)}}\ \Gamma\left(\frac{2n-1}{2n-2}\right)\ f_s(n\omega_c)}{2\pi(n-1)\ \epsilon_0\beta_1} \frac{\exp\left[in\omega_c t + i\ \frac{\pi}{4(n-1)}\right]}{t^{\frac{2n-1}{2n-2}}} \quad (32)$$

A similar analysis for the remaining two cases, $\omega_H = n\omega_c$ and $\omega_H > n\omega_c$, yields

$$E_k(x,t) = \frac{\alpha^{\frac{1}{2(n-1)}}\ \Gamma\left(\frac{1}{n-1}\right)\ f_s(n\omega_c)\ \cos\frac{\pi}{2(n-1)}}{\pi(n-1)\ \epsilon_0\beta_2} \frac{\exp\left(in\omega_c t + i\ \frac{\pi}{2}\right)}{t^{\frac{1}{n-1}}} , \quad (33)$$

for the former, and for the latter

$$E_k(x,t) = \frac{\alpha^{\frac{1}{2(n-1)}}\ \Gamma\left(\frac{2n-1}{2n-2}\right)\ f_s(n\omega_c)}{2\pi(n-1)\ \epsilon_0\beta_3} \frac{\exp\left[in\omega_c t - i\ \frac{\pi}{4(n-1)}\right]}{t^{\frac{2n-1}{2n-2}}} \quad (34)$$

4.2 $\omega = \omega_H (\neq n\omega_c)$.

The component of the electric field excited at the upper hybrid frequency is obtained by combining Eq. (22) with the k^{th} term in Eq. (29). This yields the expression

$$E_k(x,t) = \frac{f_s(\omega_H)}{2\epsilon_0}\begin{bmatrix} i\gamma_1 \\ -\gamma_2 \end{bmatrix} \exp(i\omega_H t) \int_{\Gamma_k} \frac{d\omega}{2\pi} \exp[i(\omega - \omega_H)t] (\omega - \omega_H)^{-1/2} , \tag{35}$$

where the upper bracketed entry applies for $\omega_p^2 > 3\omega_c^2$, and the lower for $\omega_p^2 < 3\omega_c^2$. Carrying out the integration along the branch cut shown in Fig. 6, and making use of the identity $\Gamma(1/2) = \pi^{1/2}$, leads to

$$E_k(x,t) = \begin{cases} \dfrac{\gamma_1 f_s(\omega_H)}{2\pi^{1/2}\epsilon_0} \dfrac{\exp\left(i\omega_H t + i\frac{3\pi}{4}\right)}{t^{1/2}} , & \omega_p^2 > 3\omega_c^2 , \\ \dfrac{\gamma_2 f_s(\omega_H)}{2\pi^{1/2}\epsilon_0} \dfrac{\exp\left(i\omega_H t - i\frac{3\pi}{4}\right)}{t^{1/2}} , & \omega_p^2 < 3\omega_c^2 , \end{cases} \tag{36}$$

4.3 $\omega = \omega_0 \ (0 < k_\perp < \infty)$.

These are the singularities discussed in Section 3.2. Substituting Eq. (27) into Eq. (28), and carrying out the branch cut integration, yields for the electric field at this resonance.

$$E_k(x,t) = \frac{2f_s(\omega_0)\cos k_0 x}{\epsilon_0[2(\partial K/\partial\omega)(\partial^2 K/\partial k_\perp^2)]^{1/2}} \exp(i\omega_0 t) \int_{\Gamma_k} \frac{d\omega}{2\pi} \exp[i(\omega-\omega_0)t](\omega-\omega_0)^{-1/2}$$

$$= \frac{2f_s(\omega_0)\cos k_0 x}{\epsilon_0[2\pi(\partial K/\partial\omega)(\partial^2 K/\partial k_\perp^2)]^{1/2}} \frac{\exp\left(i\omega_0 t + i\frac{\pi}{4}\right)}{t^{1/2}} , \tag{37}$$

where the partial derivatives are evaluated at (ω_0, k_0) .

4.4 Region of Validity.

Equations (32)-(34), (36) and (37) are valid only for sufficiently large values of time. This restriction results from expanding $K(\omega,x)$, and hence limiting our representations of $G(\omega,x)$ to small regions in the complex ω plane centered on the resonances. If the radius of one of these regions is δ_m, the corresponding branch cut integration in Eq. (28) is correct only if $t \gg (1/\delta_m)$ since the contribution from the part of the contour Γ_k outside this region will then be exponentially small. An estimate of δ_m for the resonance at $n\omega_c$, for $n\omega_c \neq \omega_H$, can be obtained from Eqs. (12) and (14). Equation (12) assumes that $|k_\perp v_t/\omega_c| \ll 1$. Hence, from Eq. (14), we must have

$$\left| 1 - \frac{1}{n^2 - 1} \frac{\omega_p^2}{\omega_c^2} \right| \frac{2^n n!}{n\omega_c} \frac{\omega_c^2}{\omega_p^2} \ll (1/\delta) \quad . \tag{38}$$

where $\delta = |\omega - n\omega_c|$. An estimate of the time for which the asymptotic results are valid is then $t \gg t_c$, where t_c is equated to the LHS of Eq. (38). A similar analysis for the other resonances yields the results:

$$t_c = \begin{cases} \left[\dfrac{2\omega_H}{(n^2 - 1)\,\omega_p^2} \dfrac{2^n n!}{n\omega_c} \right]^{1/2} & , \quad \omega = n\omega_c = \omega_H \quad , \\ \dfrac{2\omega_H}{3\omega_p^2} \left| \dfrac{\omega_p^2 - 3\omega_c^2}{\omega_c^2} \right| & , \quad \omega = \omega_H \neq n\omega_c \quad , \\ \dfrac{2\,\partial K(\omega_0, k_0)/\partial\omega}{k_0^2\,\partial^2 K(\omega_0, k_0)/\partial k_\perp^2} & , \quad \omega = \omega_0 \quad . \end{cases} \tag{39}$$

The third expression assumes $|(k_\perp - k_0)/k_0| \ll 1$ in Eq. (24).

4.5 Comparison of Resonances.

To determine the relative strengths of the resonances, we normalize E_k with respect to $E' = (f_s\omega_c^2/\epsilon_0 v_t)$. Equations (32)-(36) then become,

$$\frac{E_{k1}}{E'} = \frac{p_1}{\tau^{\frac{2n-1}{2n-2}}}, \quad \omega = n\omega_c \neq \omega_H \; ; \quad \frac{E_{k2}}{E'} = \frac{p_2}{\tau^{\frac{1}{n-1}}}, \quad \omega = n\omega_c = \omega_H \; ;$$

$$\frac{E_{k3}}{E'} = \frac{p_3}{\tau^{1/2}}, \quad \omega = \omega_H \neq n\omega_c \; ; \quad \frac{E_{k4}}{E'} = \frac{p_4}{\tau^{1/2}}, \quad \omega = \omega_0 \; . \tag{40}$$

where all phase factors have been neglected, and we have introduced,

$$\tau = \omega_c t \; , \quad p_1 = \left[2^n (n-1)! \left| 1 - \frac{1}{n^2-1} \frac{\omega_p^2}{\omega_c^2} \right|^{-(2n-3)} \frac{\omega_c^2}{\omega_p^2} \right]^{\frac{1}{2n-2}} \frac{\Gamma\left(\frac{2n-1}{2n-2}\right)}{2\pi(n-1)} \; ,$$

$$p_2 = \left[2^n (n-1)! \left(\frac{n^2-1}{2n}\right)^{2n-3} \frac{\omega_p^2}{\omega_c^2} \right]^{\frac{1}{2(n-2)}} \frac{\Gamma\left(\frac{1}{n-1}\right)\cos\frac{\pi}{2(n-1)}}{\pi(n-1)} \; ,$$

$$p_3 = \frac{1}{2\pi^{1/2}} \frac{\omega_p}{\omega_c} \left(\frac{\omega_c}{6\omega_H} \left| \frac{\omega_p^2}{\omega_c^2} - 3 \right| \right)^{1/2} \; , \quad p_4 = \frac{2}{[2\pi(\partial K/\partial\Omega)(\partial^2 K/\partial\mu^2)]^{1/2}} \; .$$

(41)

To obtain p_4, we have assumed x small so that $\cos k_0 x \approx 1$, and have introduced $\Omega = (\omega/\omega_c)$ and $\mu = (k_\perp v_t/\omega_c)$. Numerical values of p are given in Table 2. For p_4, $\omega_{n,n+1}$ indicates the passband within which the resonance lies, and has been written in this form to distinguish the specific value of ω_0 under consideration.

TABLE 2: NUMERICAL VALUES OF p .

	p_1					p_2	
(ω_p^2/ω_c^2)	n = 2	3	4	5	6	2	3
1	0.346	0.160	0.112	0.089	0.076	-	-
3	---	0.156	0.106	0.084	0.072	0	-
5	0.155	0.201	0.113	0.086	0.073	-	-
8	0.077	---	0.141	0.095	0.076	-	0.294
10	0.058	0.229	0.179	0.103	0.080	-	-

	p_3	p_4			
(ω_p^2/ω_c^2)	$\omega=\omega_H$	ω_{23}	ω_{34}	ω_{45}	ω_{56}
1	0.137	0.168	0.146	0.135	0.133
3	---	0.308	0.250	0.239	0.234
5	0.233	0.413	0.340	0.318	0.303
8	0.529	---	0.430	0.392	0.388
10	---	---	0.465	0.435	0.417

It will be seen from Eq. (40) that the decay rate at $n\omega_c$ $(n > 1)$ is critically dependent on ω_H . If $\omega_H \neq n\omega_c$, it decreases from $(1/t^{3/2})$ at $n = 2$ to $(1/t)$ as $n \to \infty$. If $\omega_H = n\omega_c$, however, the decay rates are always slower than $(1/t)$, and vary from $(1/t^{1/2})$ at $n = 3$ to a limit of a time-invariant amplitude as $n \to \infty$. When $n = 2$, Eq. (33) indicates that $E(x,t) = 0$. There is no resonance for this isolated case.

Next we compare the coefficients. Table 2 indicates $p_3, p_4 > p_1, p_2$ for $(\omega_p^2/\omega_c^2) \gtrsim 1$. Consequently, at times when Eq. (40) holds, the resonances at ω_H and ω_0 are stronger than at $n\omega_c$ $(n > 1)$. The differences may be significant. For example, for $(\omega_p^2/\omega_c^2) = 5$, the strongest resonance at $n\omega_c$ is $p_1 = 0.201$ for $n = 3$. At intermediate frequencies, ω_{34} with $p_4 = 0.34$ predominates. Thus for $\tau = 1000$, corresponding to 100 periods at the gyrofrequency, $(E_{k1}/E_{k4}) = 2.7 \times 10^{-3}$. This suggests that resonance phenomena might be more easily detected at

ω_0 and ω_H than at $n\omega_c$. The opposite is found experimentally.[4,5] The explanation is to be found in the quantity observed, which is not normally $E(x,t)$ but rather the current, $I(t)$, or voltage, $V(t)$, detected by probes. As shown by Nuttall,[10] $V(t)$ and $I(t)$ may behave differently in time. In the following section, we shall investigate these quantities. To do so, we replace the dipole source used so far by two permeable planar grids, distance a apart, oriented parallel to the magnetic field, and will compute the impedance, $Z(\omega)$, between them.

5. ASYMPTOTIC BEHAVIOR OF VOLTAGE AND CURRENT RESPONSE

5.1 Impedance, $Z(\omega)$.

The continuity equation, and the current density equation,

$$\frac{\partial}{\partial x}\left[J_{x1}(x,t) + \epsilon_0 \frac{\partial E(x,t)}{\partial t} \right] = 0 \quad , \quad J_{x1}(x,t) = - en_0 \int dv\ f_1(v,x,t) v_x \ , \tag{42}$$

must be solved together with the boundary conditions,

$$\int_{-a/2}^{a/2} dx\ E(x,t) = V(t) \quad , \quad \left[J_{x1}(x,t) + \epsilon_0 \frac{\partial E(x,t)}{\partial t} \right]_{x=-a/2} = I(t) \ , \tag{43}$$

where $V(t)$ is the voltage across the grids, and $I(t)$ is the resulting current density from the external circuit. This yields

$$E(k_\perp,\omega) = \frac{aI(\omega)}{i\omega\epsilon_0 K(\omega,k_\perp)} \left(\frac{\sin k_\perp a/2}{k_\perp a/2} \right) \ , \tag{44}$$

where we have used Fourier and Laplace transforms in space and time, respectively, and $K(\omega,k_\perp)$ is defined by Eq. (8). Inverting Eq. (44) gives,

$$\frac{V(\omega)}{I(\omega)} = \frac{a^2}{i\omega\epsilon_0} \int_{-\infty}^{\infty} \frac{dk_\perp}{2\pi} \left(\frac{\sin k_\perp a/2}{k_\perp a/2} \right)^2 \frac{1}{K(\omega,k_\perp)} \equiv Z(\omega) \ , \tag{45}$$

If either $I(\omega)$ or $V(\omega)$ are specified, we can then describe the probe response by

$$V(t) = \int_C \frac{d\omega}{2\pi} \exp(i\omega t)\ Z(\omega)\ I(\omega) \quad , \quad I(t) = \int_C \frac{d\omega}{2\pi} \exp(i\omega t) \frac{V(\omega)}{Z(\omega)} \ , \tag{46}$$

and the singularities of $Z(\omega)$ determine the asymptotic time response.

5.2 Singularities of $Z(\omega)$.

Comparison of Eqs. (10) and (45) indicates that the singularities are readily obtainable from the results of Section 3. The final expressions for $Z(\omega)$ near the singular points are as follows: For $\omega \approx n\omega_c$, multiply the RHS of Eq. (19) by $(a^2/i\omega)$. For $\omega \approx \omega_H \neq n\omega_c$, multiply the RHS of Eq. (22) by $(a^2/i\omega)$. For $\omega \approx \omega_0$, we replace $\cos k_0 x$ in Eq. (27) by $(a^2/i\omega)\,[\sin(k_\perp a/a)(k_\perp a/2)]^2$.

The asymptotic time response can now be obtained as in Section 4 by carrying out the integrations in Eq. (46) along the branch cuts.

5.3 Voltage Response, V(t) .

These results have the same temporal behavior as those of $E(x,t)$ in Section 4, and the conclusions of Section 4.5 can also be applied. The actual expressions for $V(t)$ are as follows: For $\omega = n\omega_c$, replace $f_s(n\omega_c)$ in Eqs. (32)-(34) by $[a^2 I(n\omega_c)/in\omega_c]$. For $\omega = \omega_H \neq n\omega_c$, replace $f_s(n\omega_c)$ in Eq. (36) by $[a^2 I(\omega_H)/i\omega_H]$. For $\omega = \omega_0$, replace $f_s(\omega_0)\cos k_0 x$ in Eq. (37) by $(a^2 I(\omega_0)/i\omega_0)\,[\sin(k_\perp a/2)/(k_\perp a/2)]^2$.

5.4 Current Response, I(t) .

The current behaves in a very different manner from the voltage. The expressions analogous to Eqs. (32)-(34), (36), and (37) can be shown to be,

$\omega = n\omega_c$:

$$I(t) = \frac{in\omega_c \epsilon_0 V(n\omega_c)}{a^2 \alpha^{\frac{1}{2(n-1)}}} \begin{cases} \dfrac{2(n-1)\beta_1 \sin^2 \frac{\pi}{2(n-1)}\, \Gamma\left(\frac{2n-3}{2n-2}\right)}{\pi} \dfrac{\exp\left[in\omega_c t - i\,\frac{\pi}{4(n-1)}\right]}{t^{\frac{2n-3}{2n-2}}}, & \omega_H < n\omega_c \\ \dfrac{2i(n-1)\beta_2 \sin\frac{\pi}{2(n-1)} \sin\frac{\pi}{n-1}\, \Gamma\left(\frac{2n-3}{n-1}\right)}{\pi} \dfrac{\exp(in\omega_c t)}{t^{\frac{2n-3}{n-1}}}, & \omega_H = n\omega_c \\ \dfrac{2i(n-1)\beta_3\, \Gamma\left(\frac{2n-3}{2n-2}\right)}{\pi} \dfrac{\exp\left[in\omega_c t + \frac{\pi}{4(n-1)}\right]}{t^{\frac{2n-3}{2n-2}}}, & \omega_H > n\omega_c , \end{cases} \tag{47}$$

$\underline{\omega = \omega_H (\neq n\omega_c)}$:

$$I(t) = \frac{i\omega_H \epsilon_0 V(\omega_H)}{a^2} \begin{cases} \dfrac{1}{\pi^{1/2}\gamma_1} \dfrac{\exp\left(i\omega_H t + i\dfrac{\pi}{4}\right)}{t^{3/2}}, \\ \dfrac{1}{\pi^{1/2}\gamma_2} \dfrac{\exp\left(i\omega_H t - i\dfrac{\pi}{4}\right)}{t^{3/2}}, \end{cases} \tag{48}$$

$\underline{\omega = \omega_0}$

$$I(t) = -\frac{i\omega\epsilon_0 V(\omega_0)}{a^2} \frac{\left[2\pi(\partial K/\partial\omega)\left(\partial^2 K/\partial k_\perp^2\right)\right]^{1/2}}{4\pi\left(\dfrac{\sin k_0 a/2}{k_0\, a/2}\right)^2} \frac{\exp\left(i\omega_0 t - \dfrac{\pi}{4}\right)}{t^{3/2}} . \tag{49}$$

5.5 Comparison of Current Resonances.

To determine the relative strengthsof the current resonances, we normalize $I(t)$ with respect to $I' = (\epsilon_0 v_t \omega_c V/a^2)$. Equations (47)-(49) then become,

$$\frac{I_1(t)}{I'} = \frac{q_1}{\tau^{\frac{2n-3}{2n-2}}}, \quad \omega = n\omega_c (\neq \omega_H) \quad ; \quad \frac{I_2(t)}{I'} = \frac{q_2}{\tau^{\frac{2n-3}{n-1}}}, \quad \omega = n\omega_c = \omega_H ,$$

$$\frac{I_3(t)}{I'} = \frac{q_3}{\tau^{3/2}}, \quad \omega = \omega_H (\neq n\omega_c) \quad ; \quad \frac{I_4(t)}{I'} = \frac{q_4}{\tau^{3/2}}, \quad \omega = \omega_0 , \tag{50}$$

where all phase factors have been neglected, and we have introduced

$$q_1 = 2\left[\frac{1}{2^n (n-1)!}\left|1 - \frac{1}{n^2-1}\frac{\omega_p^2}{\omega_c^2}\right|^{2n-3}\frac{\omega_p^2}{\omega_c^2}\right]^{\frac{1}{2n-2}} \frac{n(n-1)\sin^2\frac{\pi}{2(n-1)}\,\Gamma\left(\frac{2n-3}{2n-2}\right)}{\pi}$$

$$q_2 = 2\left[\frac{1}{2^n (n-1)!}\left(\frac{2n}{n^2-1}\right)^{2n-3}\frac{\omega_p^2}{\omega_c^2}\right]^{1/(2n-1)} \frac{n(n-1)\sin\frac{\pi}{2(n-1)}\sin\frac{\pi}{n-1}}{\pi}\,\Gamma\left(\frac{2n-3}{n-1}\right),$$

$$q_3 = \frac{1}{\pi^{1/2}} \frac{\omega_c}{\omega_p} \left(\frac{6\omega_H}{\omega_c} \frac{\omega_p^2 + \omega_c^2}{\omega_c^2 - 3\omega_c^2} \right)^{1/2} ,$$

$$q_4 = \frac{1}{4\pi^{1/2}} \frac{\omega_0}{\omega_c} \left[2\pi (\partial K/\partial \Omega) (\partial^2 K/\partial \mu^2) \right]^{1/2} . \qquad (51)$$

To obtain q_4 it has been assumed that $[2\sin(k_\perp a/2)/k_\perp a] \approx 1$. Numerical values of q are given in Table 3.

TABLE 3: NUMERICAL VALUES OF q .

	q_1					q_2	
(ω_p^2/ω_c^2)	n=2	3	4	5	6	2	3
1	0.921	1.059	0.951	0.853	0.776	-	-
3	---	1.083	1.005	0.904	0.820	0	-
5	2.060	0.839	0.940	0.883	0.815	-	-
8	4.120	---	0.755	0.805	0.776	-	1.405
10	5.451	0.736	0.592	0.737	0.741	-	-

	q_3	q_4			
(ω_p^2/ω_c^2)	$\omega=\omega_H$	ω_{23}	ω_{34}	ω_{45}	ω_{56}
1	1.643	3.5	5.95	8.22	10.8
3	---	2.17	3.44	4.8	6.1
5	1.675	1.79	2.69	3.66	4.18
8	---	--	2.2	2.95	3.72
10	0.998	--	2.03	2.65	3.36

Equation (50) indicates that $I(t)$ behaves in an inverse manner to $V(t)$: For $\omega_H \neq n\omega_c$, $I(t)$ at $n\omega_c$ decays slower than $(1/t)$, the rate varying from $(1/t^{1/2})$ at $n = 2$ to $(1/t)$ as $n \to \infty$. At ω_H and ω_0 , the decay is considerably faster than $(1/t)$. In particular, the decay at ω_H is as $(1/t^{3/2})$ for $\omega_H \neq n\omega_c$, and as $(1/t^{\frac{2n-3}{n-1}})$ if $\omega_H = n\omega_c$. At ω_0 the decay is as $(1/t^{3/2})$. As a

numerical example, we shall compare the resonance strengths for $(\omega_p^2/\omega_c^2) = 5$ and $\tau = 1000$. It is evident from Table 4 that the resonance current at ω_0 is two to three orders of magnitude weaker than at $n\omega_c$. The corresponding value of $(I_3(t)/I')$ for the resonance at ω_H is 5.30×10^{-5} , which is of the same order as for ω_0 .

TABLE 4: COMPARISON OF RESONANCE STRENGTHS

$(\omega_p^2/\omega_c^2) = 5$, $\tau = 1000$

n =	2	3	4	5	6
$10^3\ I_1(t)/I'$	65.1	4.72	2.97	2.09	1.63

ω =	ω_{23}	ω_{34}	ω_{45}	ω_{56}
$10^5\ I_4(t)/I'$	5.66	8.50	11.6	14.8

We should now compare these results with experimental observations. In the laboratory, Crawford, et al.,[4] observed the strongest resonances at $n\omega_c$, and a weaker resonance at ω_H . No resonances were observed at the ω_0 points. Similarly, the Alouette I records[5] show resonances at $n\omega_c$ and ω_H , but ω_0 resonances are absent. The only discordant point with our theory is the prediction that ω_0 and ω_H resonances should have approximately equal strengths. Indeed, Table 4 shows the strengths of the ω_0 resonances increasing from ω_{23} to ω_{56} . The explanation is very likely to be found in the neglect of collisional effects on the ω_0 resonances. It is illustrated elsewhere[18,19] that values of $(\nu/\omega_c) \gtrsim 10^{-3}$ have a very profound effect on K for passbands with $n \geq 2$, and $k_\perp \neq 0$.

6. RESONANCE AT THE GYROFREQUENCY

So far we have excluded the special case of resonance at ω_c . For $\omega \approx \omega_c$, Eq. (8) can be approximated by,

$$K(\omega, k_\perp) \approx - \frac{2 \exp(-\lambda) I_1(\lambda)}{\lambda} \frac{\omega_p^2}{\omega^2 - \omega_c^2} \quad . \tag{52}$$

Substituting Eq. (52) in Eq. (45) yields

$$Z(\omega) = \frac{a\, M}{i\omega_c \epsilon_0} \frac{\omega_c^2 - \omega^2}{\omega_p^2} \quad , \quad M = \frac{a}{2\pi} \int_{-\infty}^{\infty} dk_\perp \frac{(\lambda/2)}{\exp(-\lambda) I_1(\lambda)} \left(\frac{\sin k_\perp a/2}{k_\perp a/2} \right)^2 \tag{53}$$

For v_t small, $[2 \exp(-\lambda) I_1(\lambda)/\lambda] \approx 1$ and M in Eq. (53) reduces to unity. Consequently, $Z(\omega)$ has a simple zero at ω_c , and no resonance effects will occur in $V(t)$. It is evident from Eq. (46), however, that a current resonance should be expected. Evaluating the integral by residues, we obtain the following time-asymptotic component at ω_c ,

$$I(t) = \frac{\epsilon_0 \omega_p^2 V(\omega_c)}{2a\, M} \exp(i\omega_c t) \quad . \tag{54}$$

No temporal decay is indicated. The electrons are set into motion by the source function, and continue to gyrate at ω_c until such factors as collisions and magnetic field inhomogeneity cause them to dephase. Such resonances have been observed in space[5] and in the laboratory.[4]

7. DISCUSSION

In this paper, the resonant behavior of electrostatic magnetoplasma oscillations stimulated perpendicular to the magnetic field has been studied in planar geometry, for two cases. In the first of these, the electric field was determined for excitation by a dipole charge sheet. In the second, the voltage and current for excitation with parallel grids was examined. In both cases, ringing at $n\omega_c (n \geq 1)$, ω_H and ω_0 was predicted. The electric field for Case I and the voltage for Case II, have similar asymptotic time dependence and strength, which disagrees with the experimental data. The current for Case II does agree with experiment, however, in which it is effectively the current drawn by a probing antenna which is measured. The numerical results would have to be modified for cylindrical geometry, but suggest strongly that ω_H resonances should be relatively weak compared with those at $n\omega_c$. The ω_0 resonances are predicted to be as strong as those at ω_H, but the effect of even an extremely small collision frequency should be sufficient to wash these out in practice.

ACKNOWLEDGEMENTS

This work was supported by the National Aeronautics and Space Administration.

REFERENCES

1. R. W. Knecht, T. E. Van Zandt and S. Russell, J. Geophys. Res. 66, 3078 (1961).
2. R. W. Knecht and S. Russell, J. Geophys. Res. 67, 1178 (1962).
3. G. E. K. Lockwood, Can. J. Phys. 41, 190 (1963).
4. F. W. Crawford, R. S. Harp and T. D. Mantei, J. Geophys. Res. 72, 57 (1967).
5. W. Calvert and G. B. Goe, J. Geophys. Res. 68, 6113 (1963).
6. P. A. Sturrock, Phys. Fluids 8, 88 (1965).
7. W. D. Deering and J. A. Fejer, Phys. Fluids 8, 2066 (1965).
8. I. P. Shkarofsky and T. W. Johnston, Phys. Rev. Letters 15 51 (1965).
9. J. Nuttall, Phys. Fluids 8, 286 (1965).
10. J. Nuttall, J. Geophys. Res. 70, 1119 (1965).
11. J. P. Dougherty and J. J. Monaghan, Proc. Roy. Soc. 289 A214 (1965).
12. J. A. Fejer and W. Calvert, J. Geophys. Res. 69, 5049 (1964).
13. I. B. Bernstein, Phys. Rev. 109, 10 (1958).
14. R. J. Eden, 1961 Brandeis University Summer Institute, Lectures in Theoretical Physics (W. A. Benjamin, Inc., New York, 1962) 1, 1.
15. H. Derfler, Proc. Vth Intern. Conf. Phenomena in Ionized Gases, Munich 1961. (North-Holland Pub. Co., Amsterdam, 1962) Vol. 2, 1423.
16. A. Bers and R. J. Briggs, M.I.T. Elect. Res. Lab. QSR 71, 21 (1963).
17. H. B. Dwight, Tables of Integrals and Other Mathematical Data (The Macmillan Company, New York, 1967), pp. 92, 230.
18. J. A. Tataronis and F. W. Crawford, Proc. VIIth Intern. Conf. on Phenomena in Ionized Gases, Belgrade 1965. (Gradevinska Knjiga Publishing House, Belgrade, 1966) Vol. 2, 294.
19. F. W. Crawford, T. D. Mantei, and J. A Tataronis, Int. J. Elect. 21, 341 (1966).

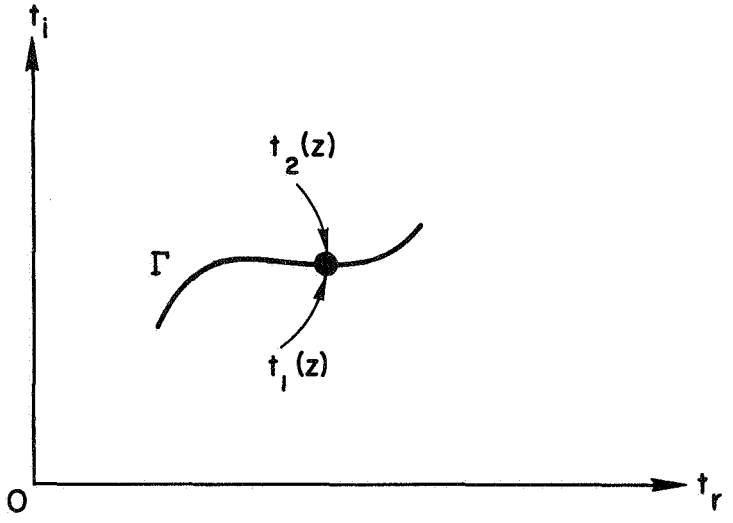

FIG. 1. SKETCH ILLUSTRATING ORIGIN OF SINGULARITIES IN $I(z)$.

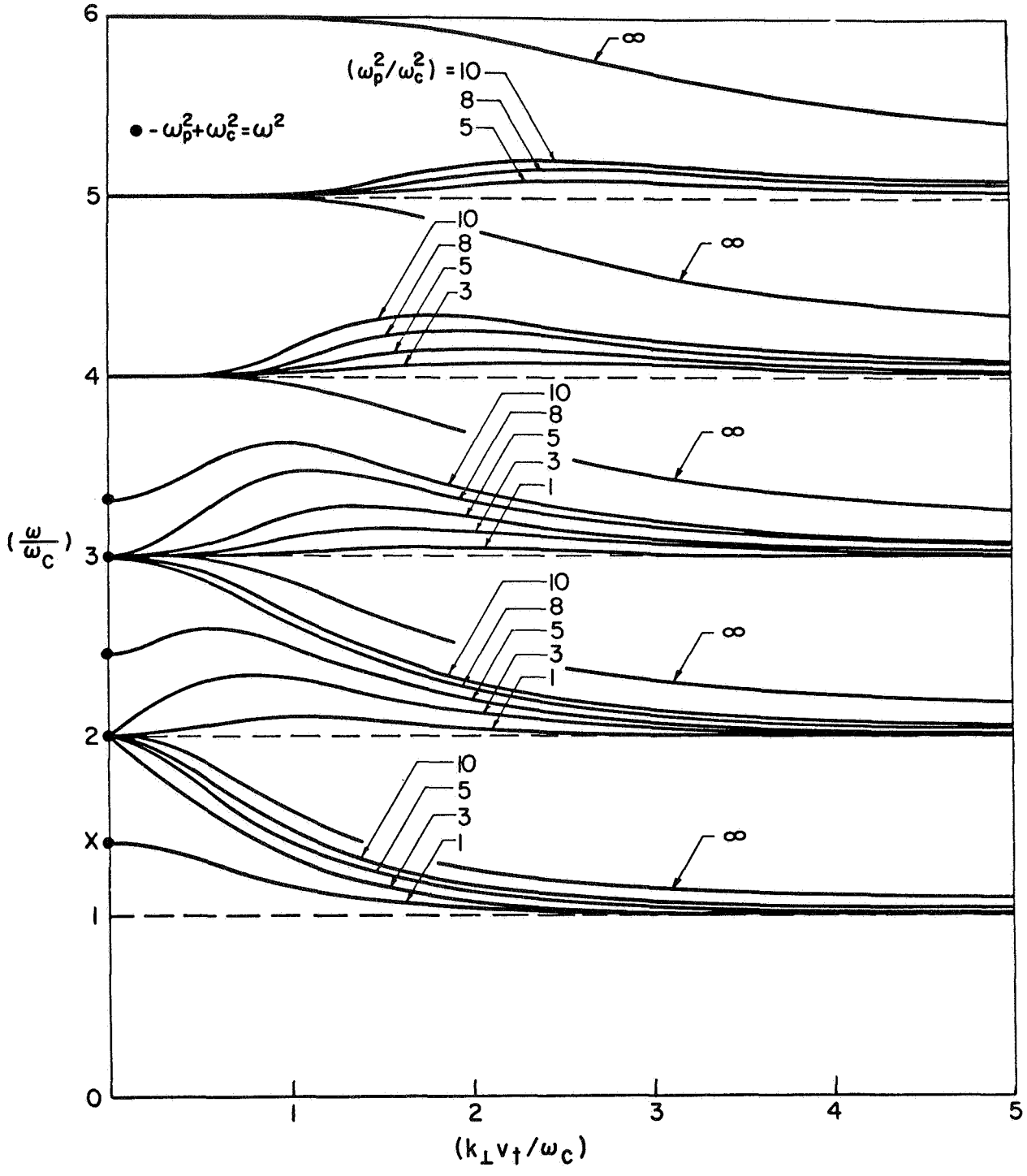

FIG. 2. DISPERSION CHARACTERISTICS OF PERPENDICULARLY PROPAGATING CYCLOTRON HARMONIC WAVES FOR A MAXWELLIAN ELECTRON VELOCITY DISTRIBUTION.

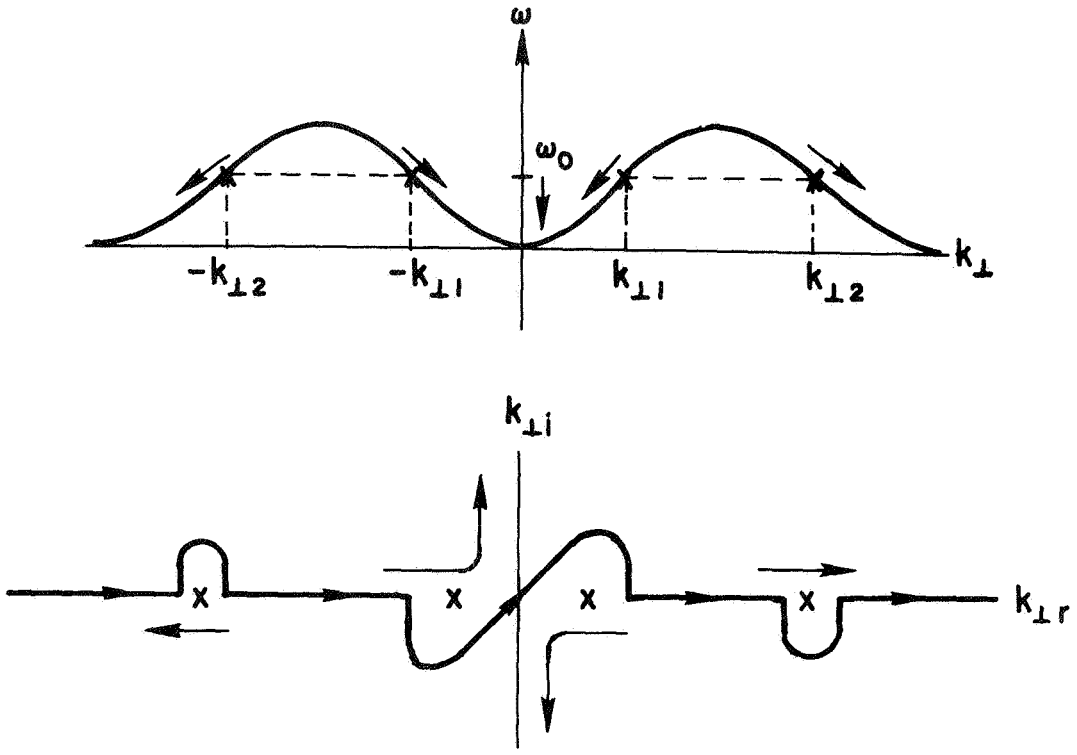

FIG. 3. CONTOUR OF INTEGRATION FOR $G(\omega,x)$ WHEN ω IS REAL.

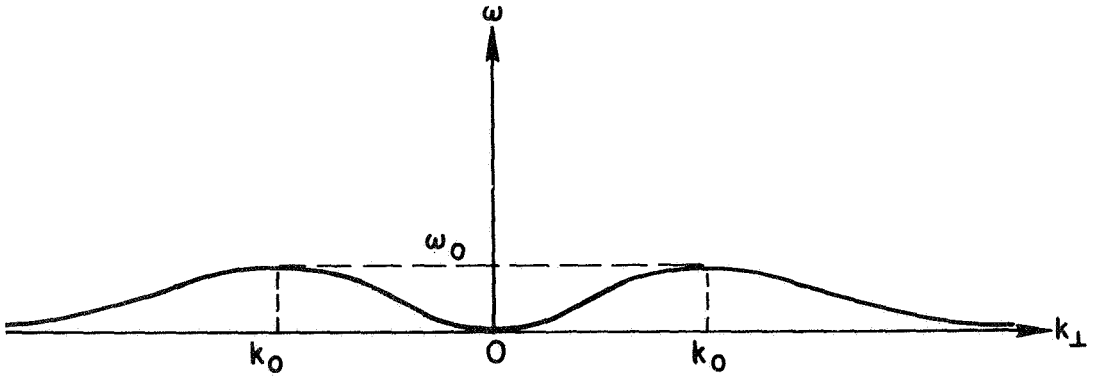

FIG. 4. PORTION OF DISPERSION DIAGRAM FOR PERPENDICULAR PROPAGATION IN A MAXWELLIAN PLASMA SHOWING POINTS WHERE THE SLOPE $(d\omega/dk_\perp)$ VANISHES FOR $0 < k_\perp < \infty$

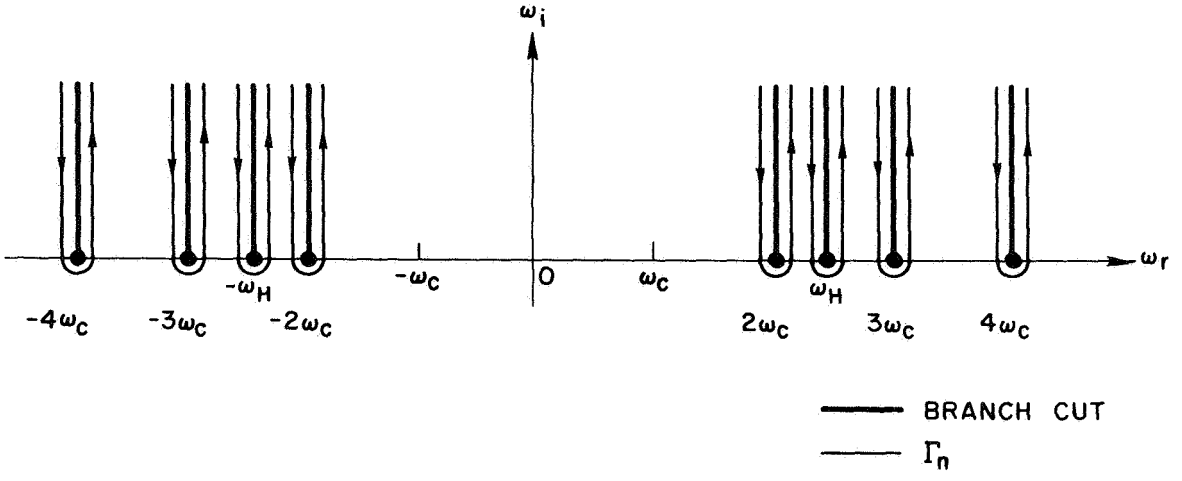

FIG. 5. CONTOUR OF INTEGRATION AROUND SINGULARITIES OF $G(\omega,x)$ (For clarity, singularities with $0 < k_\perp < \infty$ have been omitted.)

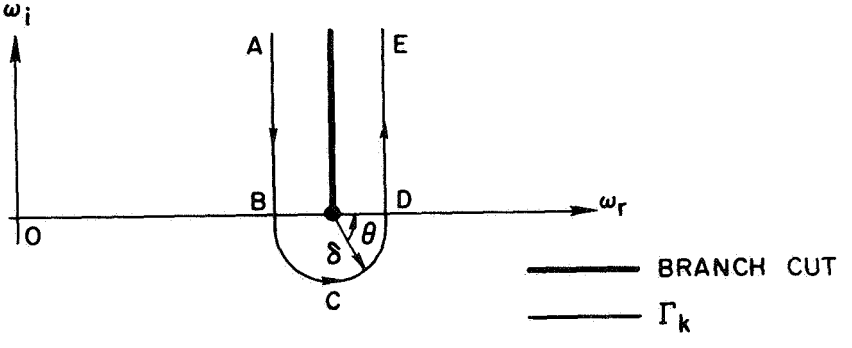

FIG. 6. CONTOUR OF INTEGRATION (Γ_k) AROUND A BRANCH-POINT OF $G(\omega,x)$.